Design and evaluation of single-phase drawbell excavation at the Chuquicamata underground mine

P. Paredes[1], F. Rodríguez[1], R. Castro[3], D. Morales[2], and D. García[2]

Affiliation:
[1]Codelco, Chile.
[2]Enaex, Chile.
[3]University of Chile- Advanced Mining Technology Center, Chile.

Correspondence to:
R. Castro

Email:
rcastro@ing.uchile.cl

Dates:
Received: 21 Mar. 2019
Revised: 7 Aug. 2019
Accepted: 10 Oct. 2019
Published: December 2019

How to cite:
Paredes, P., Rodríguez, F., Castro, R., Morales, D., and García, D.
Design and evaluation of single-phase drawbell excavation at the Chuquicamata underground mine.
The Southern African Insitute of Mining and Metallurgy

DOI ID:
http://dx.doi.org/10.17159/2411-9717/682/2020

Synopsis

The Chuquicamata Underground Mining Project (PMCHS) is one of the world's most challenging and important caving projects, as it requires the transition from one of the largest open pit mines in the world to a large-scale underground operation. In caving operations, the construction of drawbells is critical for production as these are the openings through which caved ore is extracted. The literature indicates there is no definitive blasting design methodology for drawbells when excavation is required to be completed in one phase, despite the importance and frequency of this type of requirement. Thus, during the implementation stage of the PMCHS, it was relevant to carry out an experimental programme to first design a methodology based on rock mass blasting parameters, and then conduct controlled industrial experiments to test the design's efficiency and re-engineer it accordingly. The blast design is based on the estimation of peak particle velocity (PPV) and associated damage per blast-hole. The blast sequence was defined from elemental wave analysis. Measurements during the experimental programme included drill deviation, explosive density during loading, and velocity of detonation (VOD). Drawbell geometry in one phase was successfully implemented when more than 80% of the area of the drawbell design was over four times the critical particle peak velocity (PPVc). The results obained from measurements of fragmentation and overbreak in pillars and brow during test 1 were used to improve the blasting design for test 2 so that both time and cost were reduced.

Keywords

block caving, blasting, drawbell in one phase, full-scale test.

Literature review

After a century of operation, the world's largest open pit mine will reach its profitable limit by the end of this decade. At over 1100 m in depth and 4.5 km in length, the historical Chuquicamata open pit mine will span over 11 km bottom-to-top haulage distance with an ore stripping ratio of 1:4 by 2018, leaving 4200 Mt of copper and molybdenum ore below the final open pit. In this context, block-caving methods represent the best alternative for mining the underlying massive, low-grade orebody, as these methods offer high production rates at a low cost (Araneda, 2015).

The Chuquicamata Underground Mine Project (PMCHS) is located 15 km to the north of Calama in the Antofagasta Region of Chile. Construction and development began in 2012, and production started in August 2019. At PMCHS – as for all caving mines – the proper establishment of drawbells is of crucial importance. Drawbells are the opening through which caved ore is extracted once the undercutting is completed. In the case of PMCHS, numerous drawbells will be required. For example, Lift 1 (1841) alone has over 1000 drawbells, and it is only one of three levels to be constructed. Furthermore, there are two main geotechnical domains in the orebody: the potassium east porphyry (PEK, acronym in Spanish), and quartz equals sericite (QIS, acronym in Spanish), each with different rock mass properties (Table I). Since the drawbells will be constructed in different geotechnical domains, a methodology to establish the blast design is essential.

To date, establishing drawbell design in block/panel caving has been conducted mainly through operational experience and in accordance with the mining method. In a review of drawbell geometries implemented at El Teniente between 1985 and 1994 Jofre, Yañez, and Ferguson (2000) established that at least five different designs were implemented during the life of the mine. The different designs were defined according to the mining methods used in the different sectors. Drawbells were excavated in two or three stages using ANFO as explosive and pyrotechnical detonators.

In the last few years, efforts have been made to establish drawbell excavation in a single phase in order to increase productivity (Altamirano, 2014). Silveira, Lovitt, and Hewitt (2005) indicated that the key to single-shot excavation is the use of emulsions and electronic detonators. The blasting sequence involves longer delays for the first holes (40 to 100 ms) and shorter delays at the end (5 to 20 ms) using a 1 m diameter pilot raise. Music and San Martin (2010) published results of the implementation of a single shot for large-volume drawbells at El Teniente mine. They stated that to blast a 4300 m³ drawbell, it was necessary to double the powder factor used for multiple phase drawbells and to use a raise diameter of 1.5 m for the free face. In terms of design, energy estimation contours were used to estimate the appropriate drill-hole spacing.

Dunstan and Popa (2012) summarized their experience establishing drawbells at the Ridgeway Deeps and Cadia East operations. In the case of Ridgeway, 133 drawbells were established using 14 different designs with the aim of achieving blasting in a single stage. For this, 105 holes of 76 mm diameter were charged. Two 760 mm diameter raises were used to create free surface. In the case of Cadia East, a circular design was implemented to achieve blasting in one shot without a pilot raise, using a total of 136 charged holes 76 mm in diameter. Instead of a raise, the design incorporated seven empty holes of 200 mm diameter. This methodology allowed 2100 m³ drawbells to be blasted in a single phase.

Practical knowledge on drawbell blasting and blast monitoring systems to optimize mining practices in underground and open pit operations is available in the literature (Le Juge *et al*., 1993; McKenzie *et al*., 1995; Adamson, Scherpennisse and Díaz, 1999; Hasell *et al*., 2015). However, there is a lack of published literature on blasting design methodologies for drawbell excavation in caving mines. In this study we present the results of implementing a blasting design methodology and the subsequent industrial testing carried out at PMCHS to excavate drawbells in a single phase.

Test site characteristics

The distribution of the different geotechnical units found at PMCHS is shown in Figure 1. Each of these geotechnical units has different geotechnical properties, as summarized in Table I.

Methodology

Blast design

As noted in the introduction, the literature review indicated a lack of proven blast design methodologies for drawbell excavation in one phase. An engineering criterion for drawbell blasting in one shot is that a large percentage of the excavation should be at the intense breakage threshold (at least 80%). This will ensure that the rock should is finely fragmented and can flow easily out of the drawbell. Our proposed methodology for a drawbell blasting design used this 80% criterion and included the following steps: theoretical design, implementation of the design in the field (instrumentation set-up and execution), post-blasting analysis of results, and design re-evaluation (Figure 2).

The first stage of the study consisted of blast design. The design included definitions such as drill-hole diameter, type of explosive, location of drill-holes, burden, spacing, and uncharged collar lengths. The design was based on the damage criterion. To estimate damage, it is necessary to estimate the equivalent tensile particle peak velocity (PPVc) for the rock mass:

$$PPVc = \frac{\sigma_t \times V_p}{E} \qquad [1]$$

where PPVc is the particle peak velocity (mm/s) equivalent to the tensile strength σ_t (MPa), V_p is the P-wave velocity (m/s), and E is the Young's modulus (GPa).

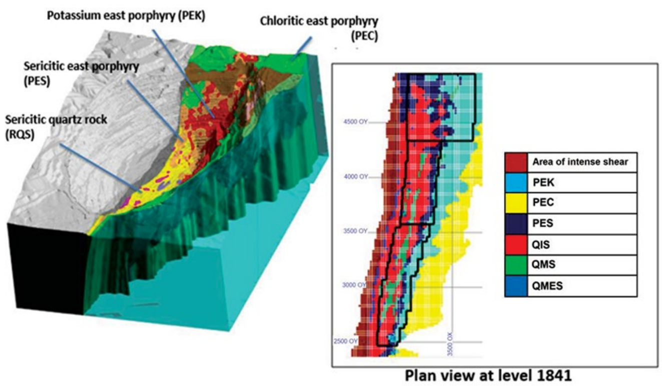

Figure 1—Geotechnical units at the Chuquicamata underground project

Table I

Geotechnical rock mass parameters

Property	PEK	QIS
Density (kg/m³)	2 610	2 700
UCS (MPa)	96.5	67.2
Tensile strength (MPa)	3.84	2.38
Young's modulus (GPa)	37.12	20.06
P-wave velocity (m/s)	5 352	4 656
Poisson's ratio	0.21	0.21
PPVc (mm/s)	551	552
4PPVc (mm/s)	2 206	2 210

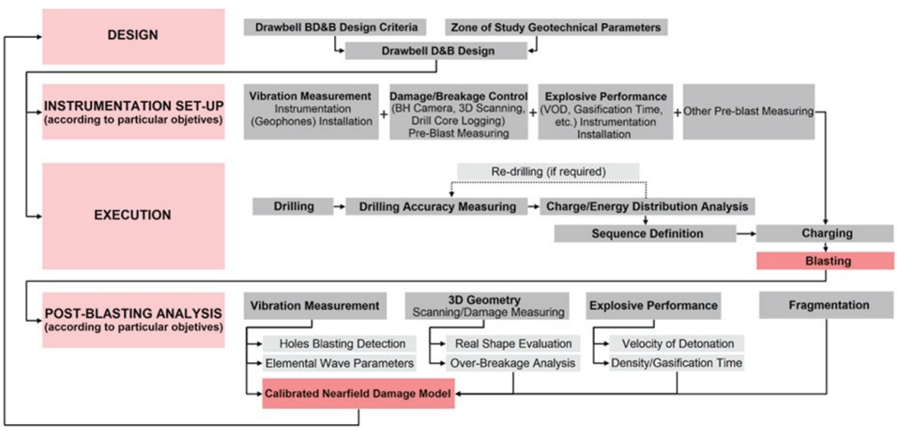

Figure 2—One-shot drawbell blast design methodology

Considering Equation [1] and the properties of the rock mass (Table I), for the rock mass at the PMCHS, the PPVc is approximately 550 mm/s. Elsewhere, intense fracturing due to blasting has been observed when the vibrations reach four times the PPVc (Adamson, Scherpennisse, and Díaz, 1999). Thus, at the PMCHS, it was expected that when the PPV reached 2200 mm/s, intense breakage of the rock mass would occur.

Once the rock mass damage criterion was determined, the next step in the design was to estimate the particle peak velocity (PPV) given the rock mass and explosive characteristics. This was achieved using the method of Persson, Holmberg, and Lee (1994) (H&P estimation):

$$PPV = kq^{\alpha}\int_{0}^{H}\frac{dh}{[Ro^2+(Rotan\emptyset-h)^2]^{\frac{\beta}{\alpha/2}}} \qquad [2]$$

where k and α are site-specific parameters, h is the charge length, Ro is the distance from the charge, $\beta = 2\alpha$, and q is the specific charge loading (kg/m). Integrating Equation [2]) to simplify conditions (Persson, Holmberg, and Lee, 1994):

$$PPVs = k * \left[\left(\frac{q}{R_o}\right) * \left(arctan\left(\frac{h+X_s-X_o}{R_o}\right) + arctan\left(\frac{X_o-X_s}{R_o}\right)\right)\right]^{\alpha} \qquad [3]$$

and abbreviating the parameters within the bracket as P

$$PPVs = k * [P]^{\alpha} \qquad [4]$$

where X_s is the uncharged drill-hole length and X_o is the depth to the point of measurement. The PPVs model was implemented in the JKSimblast software, so the estimated ground vibrations could be visualized prior to being implemented in the field (Soft-Blast, 2018). It must be noted that there are several limitations in the damage model when modelling the complexities of the detonation of explosives. However, as stated by Onederra (2013), the near field vibration approach still provides a solid basis for blasting analysis in mine engineering practice.

Implementation

The drawbell tests were conducted on two rock types at the PMCHS (Figure 2). The first blasting test was carried out in MB S02 in drawbell 22 between drives 3 and 4, where the PEK domain predominates. The second test was conducted in MB S01 in drawbell 5 between drives 3 and 4, where the QIS is predominant. These tests consisted of a single phase with a circular slot raise 1.5 m in diameter. The objective was to validate the use of the emulsion and ensure the operability of the area incorporation plan.

The drilling was carried out by an Atlas Copco Simba S7D with the positioning and drill-hole inclination using a manual system (Figure 4). The hole deviations were measured using a Boretrak deviation measurement system. This data allows real measurements of the drilled holes to be obtained from which an analysis of blasting prior to the stage of charging with explosives can be conducted. In this stage, monitoring (damage control) holes were drilled and triaxial geophones were installed in areas near the brow of the drawbell, which allowed vibration measurement in the near field (Paredes and Rodriguez, 2018), as shown in Figure 5.

With the holes drilled, the charging was carried out using a pumpable emulsion as explosive (Alcaino, Morales, and Paredes, 2018). This was done with UBS mobile equipment on a Tatra chassis, which has a telescopic loading arm to prime, load, and

Figure 4—Drilling with Simba S7D rig (Paredes and Rodriguez, 2018)

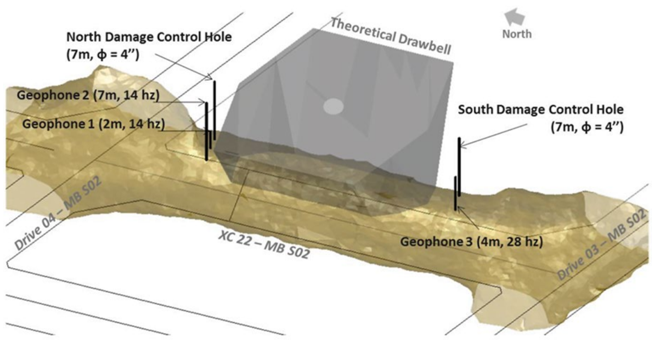

Figure 5—First drawbell trial experimental set-up (after Paredes and Rodriguez, 2018)

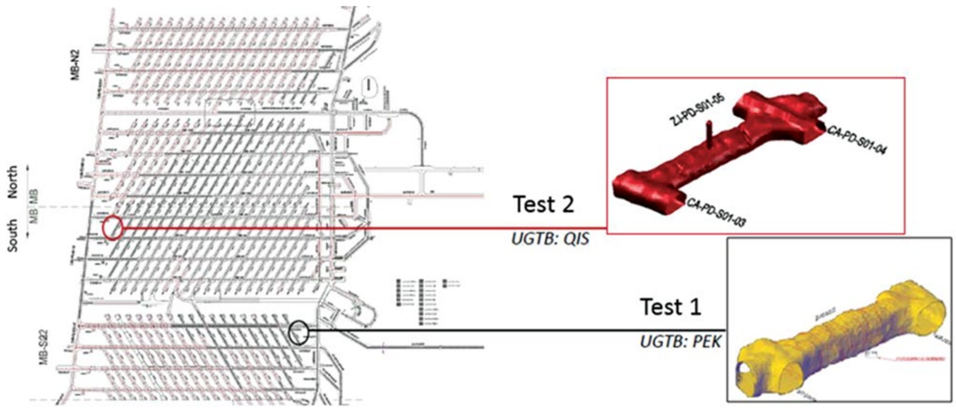

Figure 3—Location of drawbells in the PMCHS (after Paredes and Rodriguez, 2018)

install the stemming. The control and measurement of densities of the final product was carried out during the loading of the explosive with the mobile UBS unit in the gasification process. Control of the gasification time was done at 10 minute intervals until reaching 60 minutes of charging.

To establish the detonation sequence, the elementary wave theory was applied, which uses the effect of the linear superposition of the waves generated by the detonation of different explosive charges in a blast (Enaex, 2011). With this method, the delays between holes that generate a maximum level of stress in the blast and minimize the damage in the far field could be determined, thus avoiding the coupling between charges.

For velocity of detonation (VOD) measurements, an RG-6 coaxial cable within two holes at the central rings and ShotTrack explosive detonation velocity measurement equipment were used. The monitoring and programming were then completed, and the test concluded with drawbell blasting.

After blasting, post-blasting test analysis was carried out. The results analysed included the fragmentation observed in the blasting pile, vibration measurements in the near field, and a 3D scan of the final geometry of the drawbell. Finally, the design was re-evaluated to optimize it according to the results obtained and the operational requirements.

Drawbell 1 blasting test

Design

The blast design of the first drawbell included sixty 76.2 mm diameter drill-holes distributed in nine rings with a 1.5 m slot raise. Table II shows the main parameters associated with the drawbell 1 blasting design, while Figure 6 shows the location of the drill-holes.

The assessment of the design in the JKMRC software indicated that for a plan view located at the mid-height of the drawbell, the estimated area of intense fracturing reached 84% (Figure 7). Therefore, it was expected that the drawbell could be excavated in a single shot.

Drilling

After drilling, measurement of hole length and deviation indicated that 5% of the holes were shorter than the design parameter specified, 55% were within the design parameter, and 40% were longer than the design parameter for a tolerance of 0.5 m (Figure 8). After a charge distribution analysis, the addition of new drill-holes was dismissed.

Table II

First drawbell – blast design parameters

Parameter	Value
Drawbell volume (m³)	1 181
Drawbell height (m)	9
Slot raise diameter (m)	1.5
Hole diameter (mm)	76.2
Spacing (m)	1.7–2.4
Burden (m)	1.9
No. of holes	60
Drilling metres (m)	569
Drilling factor (m/m³)	0.63
Powder factor (kg/m³)	2.66
Powder factor (kg/t)	1.05

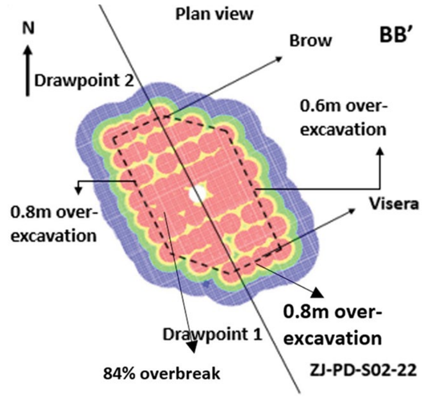

Figure 7—Damage contour for blast design for the first drawbell

Charging

Charging was carried out with mechanized equipment using gassed pumpable emulsion, which is normally used for intermediate diameter holes (Figure 9). It has a high water resistance, good adherence, and high VOD. The sensitization was done *in-situ* through a gasification process to obtain the gassed bulk pumpable emulsion explosive agent.

The total amount of explosives was 2335 kg using 60 detonators (one 250 g High Detonation Power explosive for each drill-hole), with a powder factor of 2.55 kg/m³. Density control and measurement of the final product was performed during the explosive charging with the UBS mobile unit to reach a final density of 1 150 ± 5% kg/m³ in the gasification process. The gasification time was controlled in intervals of 10 minutes

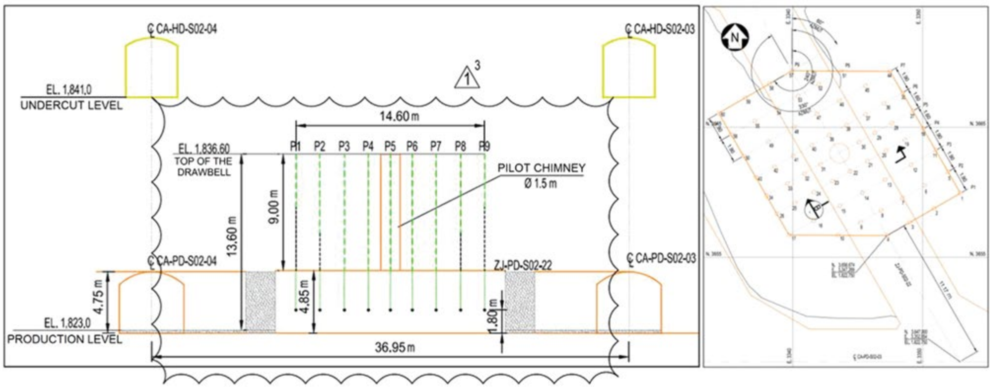

Figure 6—Drawbell 1 design section and plan view (Paredes and Rodriguez, 2018)

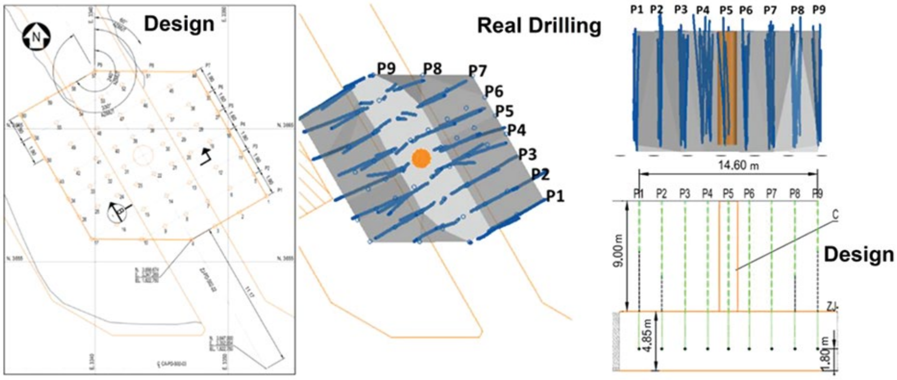

Figure 8—3D plan and section view of actual drilling *vs* theoretical drilling (after Paredes and Rodriguez, 2018)

Figure 9—ShotTrack cable and charged holes (Paredes and Rodriguez, 2018)

Table III **Gassed pumpable emulsion: technical characteristics**	
Density (kg/m³)	1 150 ± 5%
Velocity of detonation (m/s)	4 000 – 5 000
Detonation pressure (MPa)	6 000
Energy (kJ/kg)	2 847
Volume of gases (L/kg)	1 000
Critical diameter (m)	0.38
Resistance to water	Good
RWS	0.79
RBS	1.17

up to 60 minutes. Figure 10 shows that in 40 to 50 minutes the explosive reached the required density within the expected ranges.

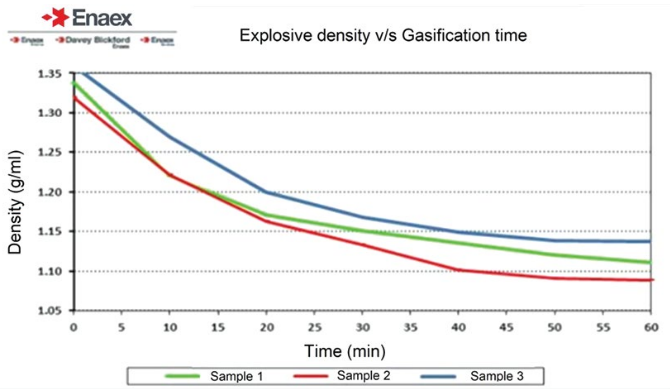

Figure 10—Explosive density *vs* gasification time

The measurements of VOD were made in the central holes 39 and 47, which correspond to rings 6 and 7. Figure 11 shows a measurement scheme and the VOD registered as being within its technical characteristics (Table IV).

Sequence

The detonation sequence and delay times are shown in Table IV and Figure 12. A short sequence with delays of 25 ms between charges was used for the first four central holes (stage 1 in Figure 12). A time lag of 100 ms was introduced to allow for the evacuation of the blasted rock in the central zone. This was followed by delays of 25 ms in a helical direction to form the

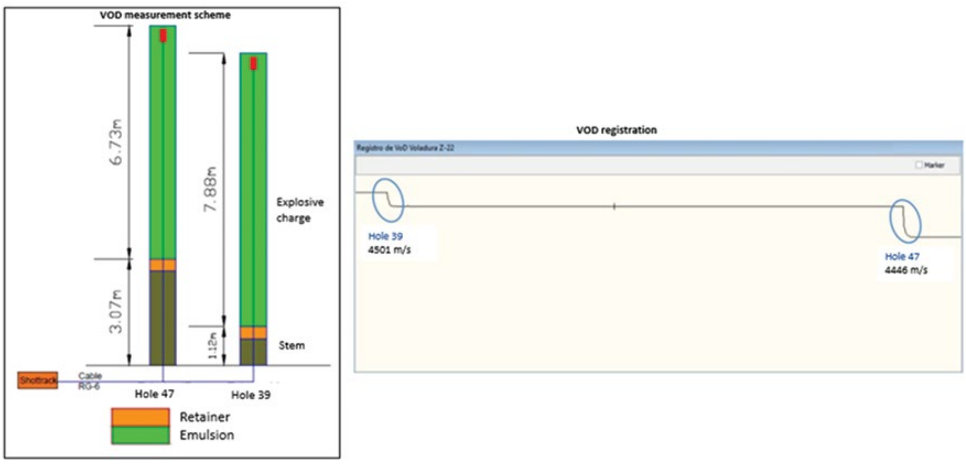

Figure 11—VOD measurement scheme (left) and VOD registration (right)

Table IV

Time delay characteristics for test 1

Parameter	Value
Total time (ms)	1 800
Initial time delay (ms)	25
Interval (ms)	100
Final time delay (ms)	50
Average charge per delay (kg)	39
Maximum charge per delay (kg)	52

complete geometry of the rings P3 through P7 (stage 2). Finally, the rings P1, P2, P8, and P9 were detonated with delays of 50 ms (stage 3).

Near field vibration measurements

The instrumentation consisted of three triaxial geophones, two of which were located on drift 4 and the third on drift 3 (Figure 13). A vibration database was obtained with a total of 180 measurements (60 measurements per geophone, Figure 14).

With the vibration records, an adjustment was made to Equation [4] using the total set of vibration data. As noted in Figure 15, the blast constants k = 189 and α = 0.9 were estimated with a correlation coefficient of 0.53 with respect to the observed data. Additionally, the P-wave velocity for the rock mass was estimated to reach 5330 ± 258 m/s, which is consistent with the rock mass characteristics shown in Table I.

To establish the minimum delay between charges and avoid coupling of vibrations at the brow, a wave period analysis (δ_t) was conducted. This indicated that 90% of the measured vibrations had a period below 7.7 ms. The minimum time between charges T_{min} is calculated as

$$T_{min} = \delta_t + \frac{D_{max}}{V_p} \qquad [5]$$

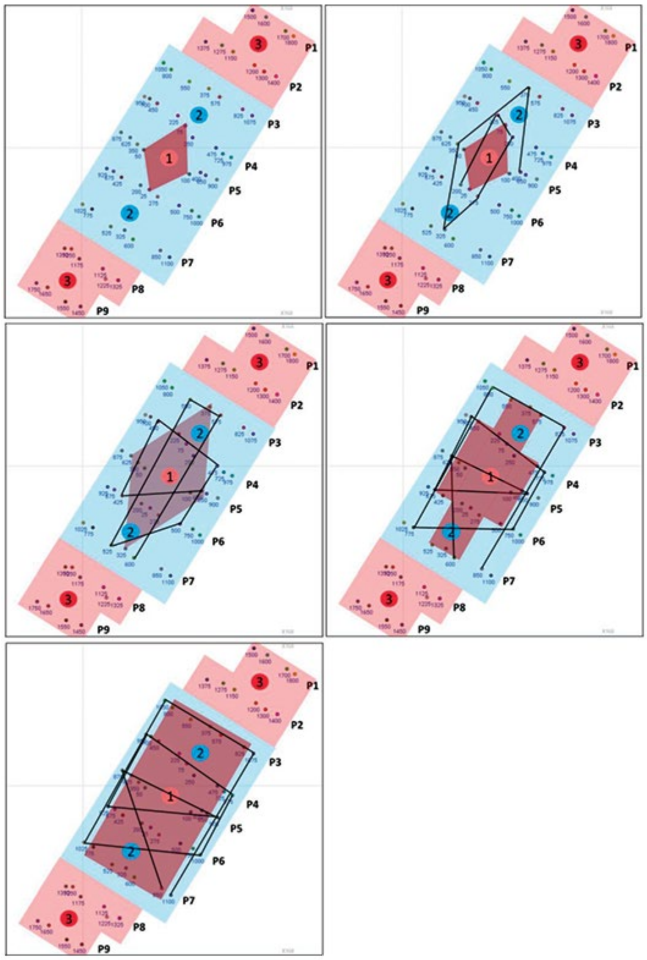

Figure 12—Blasting sequence showing stages 1 to 3 (Paredes and Rodriguez, 2018). Stage 1 delays of 25 ms, delays of 100 ms between stages 1 and 2, stage 2 in helical direction with delays of 25 ms, and finally stage 3 delays of 50 ms

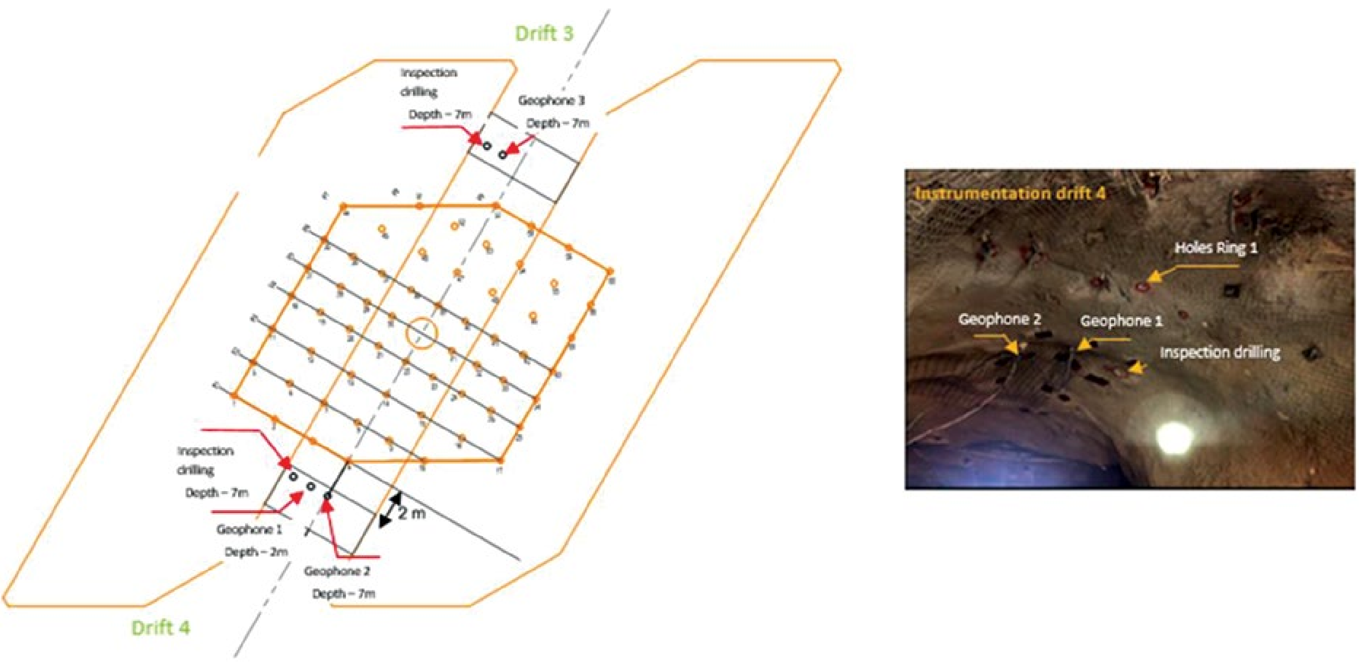

Figure 13—Instrumentation for vibration measurement

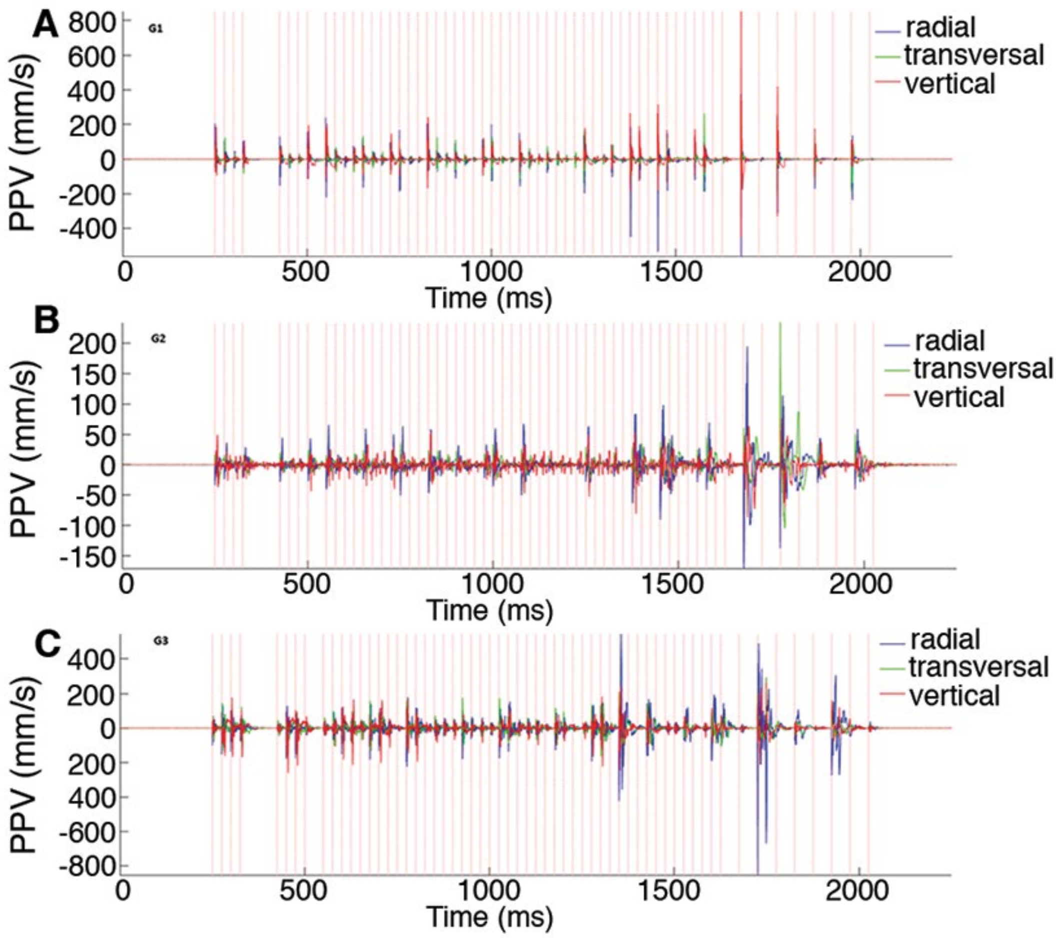

Figure 14—Vibration registered by (A) geophone 1, (B) geophone 2, and (C) geophone 3 (Paredes and Rodriguez, 2018)

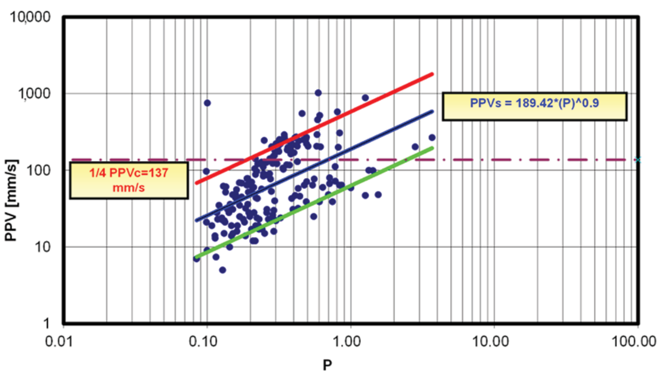

Figure 15—H&P adjustment from near field vibration data, where *P* is the term defined in Equation [4]

where D_{max} is the maximum distance to the brow (19.9 m). Thus T_{min} reached 11.4 ms.

Fragmentation measurements

The fragmentation obtained from the blasting was analysed through image analysis from both sides of the drawbell (drives 3 and 4). Figure 16 shows the photographic record for the fragmentation analysis, while Figure 17 shows the size distribution curve obtained. As noted, the fragmentation could be considered as fine: the maximum size does not exceed 803 mm and the d_{80} is between 307 mm and 325 mm.

Drawbell geometry results

After drawing the blasted rock, a 3D scan of the geometry of the drawbell was made using the I-Site system (Figure 18).

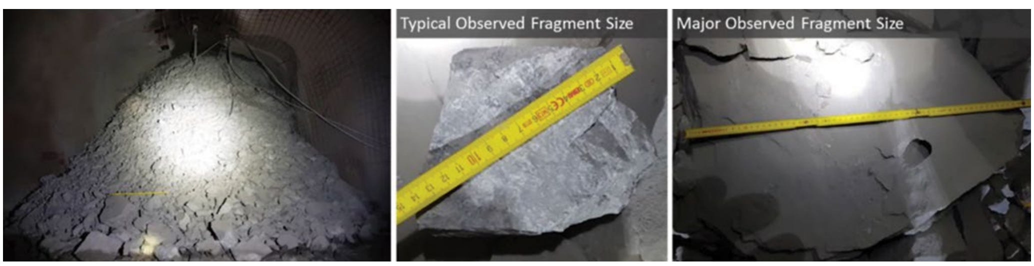

Figure 16—Post-blast results (after Paredes and Rodriguez, 2018)

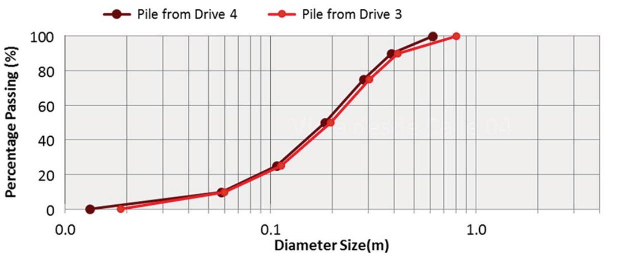

Figure 17—Fragmentation curves for piles measured from both sides (drives 3 and 4)

Figure 18—I-Site scanning (Paredes and Rodriguez, 2018)

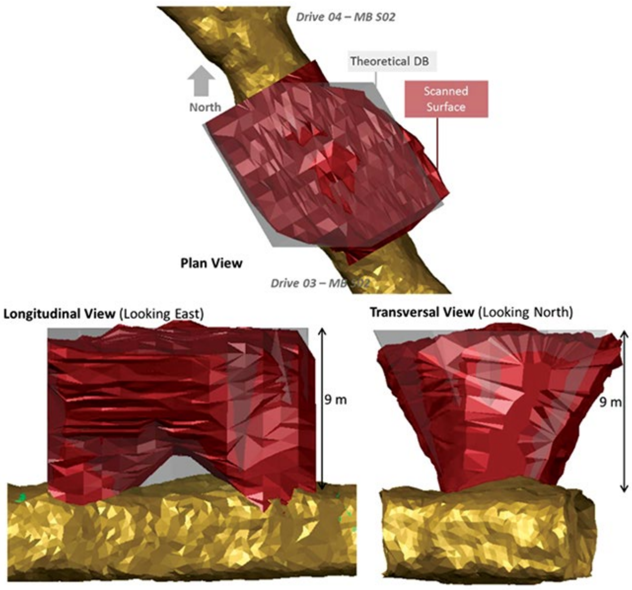

Figure 19—Scanned surface and theoretical drawbell (after Paredes and Rodriguez, 2018)

Figure 19 shows the resulting geometry. In general terms, the drawbell geometry was achieved with minor damage on the perimeter, which was expected from the design phase. Finally, the pre- and post-borehole camera inspection of damage control holes indicated there was no observable damage in the brow pillar.

Drawbell 2 blasting test

Design

To optimize the previous design, and after an analysis based on the H&P calibrated model, the 60 holes used in the drawbell 1 test were reduced to 48 holes in the drawbell 2 test while maintaining the 0.5 m offset in order to protect the brow (Figure 20). Furthermore, because the fragmentation in the first test was finer than required, a design was applied with a powder factor of 0.88 kg/t, compared with the 1.05 kg/t used in drawbell 1 (Table V). This resulted in 100 m less drilling to achieve the same objective.

Figure 21 shows a plan view of the estimated damage and overbreak in the drawbell. It was estimated that the design would achieve 83% intense breakage of the rock mass. This meant that it would be possible to excavate in one phase with fewer drill-holes. In terms of damage, some minor overbreak was expected to occur in the minor apex and no overbreak on the brow.

Drilling

Once the holes were drilled, measurements of deviations and achieved lengths were conducted (Figure 22). After a charge

Table V

Design parameters, drawbell 2

Parameter	Value
Drawbell volume (m³)	1181
Drawbell height (m)	9
Slot raise diameter (m)	1.5
Hole diameter (mm)	76.2
Spacing (m)	2.5–2.6
Burden (m)	1.6–1.8
No. of holes	48
Drilling metres (m)	466
Drilling factor (m/m³)	0.51
Powder factor (kg/m³)	2.0
Powder factor (kg/t)	0.88

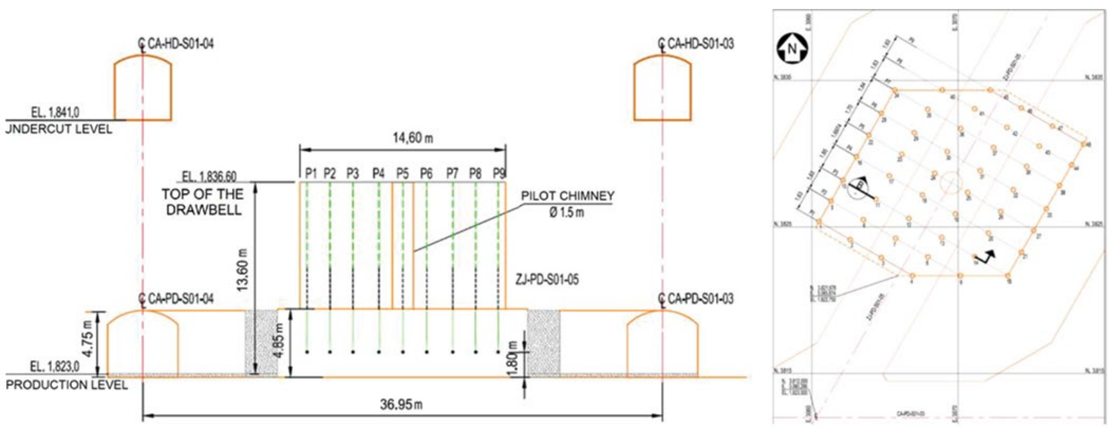

Figure 20—Drill-hole distribution and design, drawbell 2 (Paredes and Rodriguez, 2018)

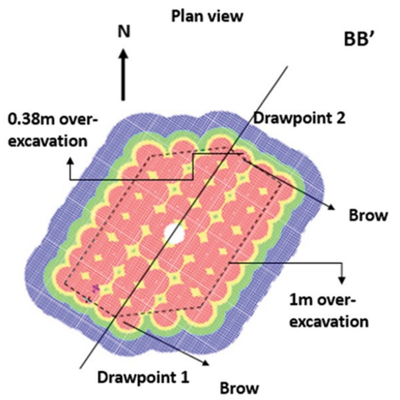

Figure 21—Plan view of the drawbell 2 simulation – section at the middle of the drawbell

distribution analysis, it was noted that the deviation of the E-W contour holes at rings 5 and 6, as well as short holes at rings 7, 8, and 9 could imply low charge concentration areas. In response to this possibility, the short holes of rings 7, 8, and 9 were re-drilled and two auxiliary holes at rings 5 and 6 were added.

Sequence

The detonation sequence consisted of delays of 20 ms for the first six central holes followed by a lag of 100 ms to the next holes and continuing with 20 ms delays in a helical direction to form the complete geometry of rings 4 to 6. Finally, to minimize damage to the brow, lags of 100 ms were applied to rings 1, 2, 3, 7, 8, and 9.

Charging

The explosive reached a density of 1.15 g/cm^3, and the total charge was 1898 kg of explosive, which is 19% less than the case of test 1, with a powder factor of 2.1 kg/m^3. APD 250-Ballistic and plastic retainer were used under the same loading methodology. Charging was completed in 3 hours and 35 minutes, 38 minutes less than the loading in drawbell 1. The VOD measurements were made in holes 25, 31, and 39, corresponding to rings 5, 6, and 7. An average VOD of 4450 m/s was obtained for hole 25, 4627 m/s for hole 31, and 4153 m/s for hole 39, which gives an average of 4410 m/s for the explosive agent.

Fragmentation results

Figure 24 shows the fragmentation of blasted material. As noted, the blast was conducted after the installation of a beam located at the brow to contain the broken rock. There was no observable damage to infrastructure, nor displacement of the brow beam (confirmed with topographic measuring). Fragmentation was coarser than in test 1 but could easily be handled by the loading system.

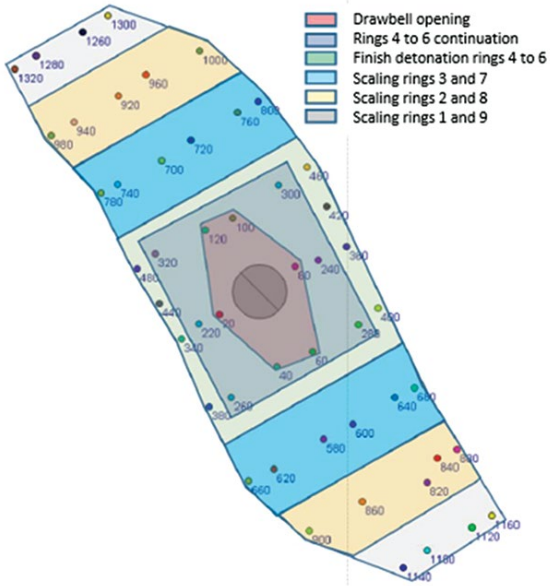

Figure 23—Detonation sequence, test 2

Table VI

Time delay for test 2 and amount of explosive per delay

Parameter	Value
Total time (ms)	1 320
Time delay (ms)	20
Interval 1, 2, and 3 (ms)	100
Average charge per delay (kg)	39
Maximum charge per delay (kg)	53

Figure 24—Blasted material pile in drifts 3 and 4. drawbell 2 (Paredes and Rodriguez, 2018)

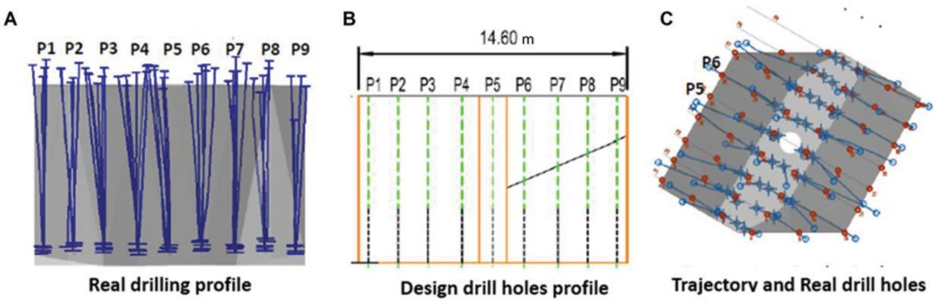

Figure 22—Sections showing actual and design drill-holes. (A) Side view of the actual drilling profile with drill deviation, (B) side view of the design drilling profile, (C) plan view of the actual drilling profile and trajectory (based on Paredes and Rodriguez, 2018)

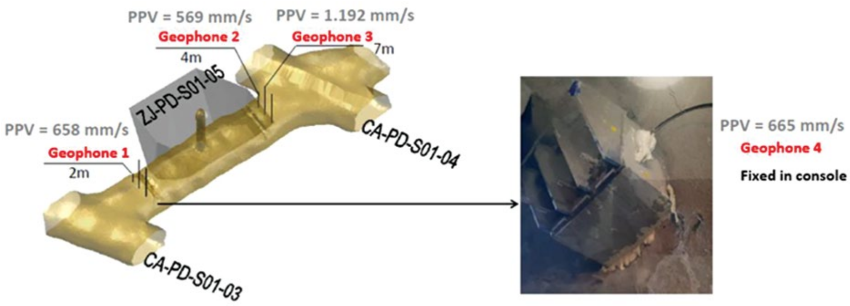

Figure 25—Instrumentation and installation of geophones, drawbell 2 (after Paredes and Rodriguez, 2018)

Near field vibration measurement

The installation configuration of the geophones with the maximum PPV obtained is shown in Figure 25. The maximum recorded PPV reached 1192 mm/s in geophone 3 at 7 m above the roof of the drift (similar to the maximum PPV reached in the first drawbell (test 1) of 1024 mm/s), while the maximum PPV measured in the brow beam console was 665 mm/s.

Conclusions

In this study we established and tested a practical methodology for continuous improvement of a drawbell design. To this end, a theoretical design was first established, followed by two blast tests conducted to validate the design assumptions.

The importance of instrumentation and measurement for understanding the behaviour of design and operational parameters is highlighted, as it allows decisions to be made based on empirically tested data, thus minimizing risk and enabling continuous improvement.

Drawbell blasting in one phase was found to be possible when more than 80% of the area of the drawbell is over four times the PPVc limit, ensuring an optimal blast-hole interaction with drawbell geometry. While this is an engineering-based criterion, further fundamental research is required to understand the mechanisms involved.

The results indicate that both tests were implemented successfully, using emulsion and electronic detonators for two different sets of rock mass characteristics. Although the rock masses tested were different, the PPVc values in both were similar, as shown in Table I. Therefore, the rock masses' response to blasting were expected to be similar as well. The success of the implementation was measured in terms of operational factors such as time for setting the explosive, fragmentation, near field vibration, and the final drawbell geometry.

Using two controlled tests allowed lessons learned from test 1 to be applied in test 2 to increase efficiency in terms of time and cost and to improve the overall design using a methodology that could be applicable to other underground mines.

Acknowledgment

The authors would like to thank Codelco for their permission for this work to be published. R. Castro would like to acknowledge the contributions of Juan Henriquez and Alvaro Altamirano at different stages during this research.

References

Adamson, W.R., Scherpennisse, C.R., and Díaz, J.C. 1999. The use of blast monitoring/modelling systems for the optimization of development systems. *Proceeding of Explo '99*, Kalgoorlie, Australia, 7-11 November 1999. Australasian Institute of Mining and Metallurgy, Melbourne. pp. 35–42.

Alcaino, J., Morales, D., and Paredes, P. 2018. Implementación de emulsión en desarrollos horizontales, PMCHS. *Proceedings of UMINING 2018, II Congreso Iberoamericano en Minería Subterránea y a Cielo Abierto*. Santiago, Chile, 13–15 June 2018. Castro, R. and Herazo, Y. (eds). pp. 438–451.

Altamirano, A. 2014. Design of blasting in one phase- application to the Continuous Mining Project, Andina Mine. Masters rhesis, University of Chile, Santiago [in Spanish].

Araneda, O. 2015. Challenges and opportunities in open pit to underground transition at the Chuquicamata Underground Mine Project. Keynote presentation: *Mine Planning 2015 Conference*, Antofagasta, Chile, 8–10 July 2915.

Dunstan, G. and Popa, L. 2012. Innovative cave establishment practices at Ridgeway Deeps. *Proceedings of the Sixth International Conference & Exhibition on Mass Mining*, Sudbury, Ontario, Canada. Canadian Institute of Mining, Metallurgy and Petroleum, Montreal.

Enaex. 2011. El modelo de onda elemental. Software SeedWave. Herramienta integral para el control de daño en el campo cercano y lejano. Santiago, Chile.

Hasell, R., Villaescusa, E., de Vries, R., and Player, J. 2015. Stope blast vibration analysis at Dugald River underground mine. *Proceedings of the 11th International Symposium on Rock Fragmentation by blasting*, Melbourne, Australia, 24–26 August 2015. Australasian Institute of Mining and Metallurgy, Meburne. pp. 221–232.

Jofre, J., Yañez, P., and Ferguson, G. 2000. Evolution in panel caving undercutting and drawbell excavation, El Teniente Mine. *Proceedings of MassMin 2000*, Brisbane, Australia, 29 October – 2 November 2000. Australasian Institute of Mining and Metallurgy, Melbourne. pp. 249–260.

Le Juge, C.E., McKenzie, C.K., Simpson, J., and Stewart, R.S. 1993. Blast control in small scale underground mining. *Proceedings of the Narrow Vein Mining Seminar*, Bendigo, , Australia, 17–18 June 1993. Australasian Institute of Mining and Metallurgy, Melbourne. pp. 65–70.

McKenzie, C., Scherpenisse, C., Arriagada, J., and Jones, J.1995. Application of computer assisted modelling to final wall blast design. *Proceedings of the Explo 95 Conference*, Brisbane, Australia, 4–7 September 1995. Australasian Institute of Mining and Metallurgy, Melbourne. pp. 285–292.

Music, A. and San Martin, J. 2010. Great volume drawbells at El Teniente. Internal Report. CODELCO, Division El Teniente.

Onederra, I. 2013. Blast damage modelling and assessment. Course Notes. CRC Mining, University of Queensland.

Paredes, P. and Rodriguez, F. 2018. Methodology, execution and results of the first drawbell blasting in a single shot trial in PMChS. Internal Report. CODELCO.

Persson, P.A., Holmberg, R., and Lee, J. 1993. Rock Blasting and Explosives Engineering. CRC Press.

Silveira, A.C., Lovitt, M., and Hewitt, T. 2005. Off to a good start with Lift #2: Drawbell extraction - Norhparkes. *Proceedings of the Ninth Underground Operators' Conference*, Perth, Australia, 2005. Australasian Institute of Mining and Metallurgy. pp. 75–80.

Soft-Blast. 2018. JKMRC JKSimblast software description. https://www.soft-blast.com [accessed November 2018]. ◆